Reinforced concrete beam analysis supplementing concrete contribution in truss models

Li, Bing.; Tran, Cao Thanh Ngoc.

2008

Li, B., & Tran, C. T. N. (2008). Reinforced concrete beam analysis supplementing concrete contribution in truss models. Engineering Structures, 30 (11), 3285-3294.

https://hdl.handle.net/10356/95999

https://doi.org/10.1016/j.engstruct.2008.05.002

Reinforced concrete beam analysis supplementing concrete contribution in truss models

Bing Li *, Cao Thanh Ngoc Tran

School of Civil and Environmental Engineering, Nanyang Technological University, Singapore

**Corresponding author: E-mail address: cbli@ntu.edu.sg (B. Li).*

Abstract:

A truss model is presented in this paper to predict the load–deflection response of reinforced concrete beams subjected to flexure and shear. The truss model which has struts at various angles is derived considering concrete contribution. The concrete contribution is then integrated into the modified truss model through the concept of equivalent stirrup reinforcement. The validity and applicability of the proposed truss model is evaluated by comparing results with experimental data. Good correlations with the experimental data have been obtained. This study shows that the truss model analogy, if properly treated, can be used to access both shear strength as well as the load–deflection response of reinforced concrete elements subjected to shear and flexure.

Keywords:

Reinforced concrete beam

Concrete contribution

Truss model

Shear

1. Introduction

It is common to use concrete to carry compressive forces and steel reinforcement to carry tensile forces in flexural design of reinforced concrete (RC) beams. This idea was further developed into the concept of a truss analogy utilizing concrete blocks as compression struts to resist compressive forces and reinforcing bars as tension ties to carry tensile force. The truss analogy, which is based on relevant experimental evidence, assumes that inclined cracks form in RC beams at failure. The concrete stress blocks between adjacent cracks would carry the inclined compressive forces and

act as diagonal compression struts. This led to the realization that a truss-like action could be achieved through longitudinal reinforcement representing the tensile chord of the truss while the concrete represents the compressive chord on either side of the beam, and then stirrups to provide vertical tension ties joining the adjacent longitudinal chords. Such a truss model analogy has greatly influenced the shear design procedure for determining ultimate shear capacities of RC beams throughout the years. Moreover, its visible nature allows it to represent the shear failure mechanism, through which many analytical models have been developed. These models aid in the analyses of stiffness and deformation of RC elements. Significant contributions have been made by many researchers to the development of truss models of RC beams subjected to shear and flexure.

Bresler and MacGregor [1] reviewed the mechanism and analyses of RC beams which failed in shear and gave graphical illustrations based on a classical truss model. This provides an initial concept for the modified truss model with struts at various angles. In this model, the chords are assumed to be parallel to each other. All shear must be carried by tension in the transverse reinforcement as neither chord can transmit any transverse load. However, to account for the experimentally observed shear capacity of concrete in a beam (with and without reinforcement), it may be assumed that the compression chord of the truss is curved. This is then known as the modified truss model. Although further analytical work on these models was not available at that time, they gave a very good conceptual basis for further research on truss model analogy.

Paulay [2] found that shear deformation was developed due to truss action when estimating deformations of coupling beams after cracking. A considerable portion of shear force was found to transfer from one support to the other through a truss formed by the stirrups and the diagonal concrete strut. An analogous truss model with tapered struts was used by Paulay [2] to study the principal dimensions of the compression struts and deformation of a typical shear transfer linkage. Then from the compatibility condition, shear rotation of the analogous variable angle truss model was determined. Paulay's work laid the solid foundation for further detailed analysis with the truss model analogy.

Recently, To et al. [3] attempted to develop strut-and-tie model formation procedure, which

allowed the cyclic hysteretic response of RC structures to be examined. For this purpose, an idealized uniaxial fiber model was proposed to simulate the axial force–displacement characteristic of a combined concrete and steel reinforcing element. The model was subsequently employed as the top and bottom longitudinal chord members in the strut-and-tie model. The dimensioning of chords struts and ties and allowable strength of these members were briefly discussed too. The strut-and-tie model obtained from their suggested procedure gave satisfactory analytical results to the experimental evidences. However, the suggested procedure was simple and thus resulted in several deficiencies in the prediction.

As reviewed earlier, truss model analogy demonstrated its convenience and potential in analyzing strength and deformation of RC structural members. The Current ACI 318 [4] design code also comments that requirement for serviceability besides the ultimate limit state should be complied when using the truss model analogy for design. Thus, there is a need to investigate strength and deformation of RC elements when modeled by the truss analogy. The objective of this paper is to propose an analytical truss model with struts at various angles, capable of tracing the response of RC beams subjected to shear and flexure.

Notations

a	Shear span length or depth of the equivalent rectangular stress block
a'	Depth of the transformed equivalent rectangular tress block
A_{cm}	Sectional area of compression chord
A_s	Sectional area of longitudinal reinforcement
A_{sc}	Sectional area of stirrup reinforcement converted from concrete contribution
A_{sm}	Section area of diagonal strut
A_v	Sectional area of shear reinforcement
b	Beam total sectional width
b''	Width of confined core measured to outside of stirrups
c	Distance from extreme compression fiber to neutral axis
C_c	Resultant of concrete compression force
C_s	Resultant of reinforcement compression force
d	Effective depth of the beam taken from the extreme compression fiber to the centroid of the outermost layer of tension reinforcement
f_c	Concrete compressive stress
f'_c	Cylinder strength of concrete
f_s	Stress of tensile reinforcing steel bar
f'_s	Stress of compressive reinforcing steel bar
f_y	Yielding stress of reinforcing steel bar
h	Height of truss
jd	Flexural lever arm
l_b	Critical strut length
s	Spacing of stirrups
T	Resultant tensile force
V_c	Truss contribution
V_s	Stirrup contribution
Z	Slope of descending branch for confined concrete in the stress–stain relationship
α	Strut angle
ε_c	Concrete strain
ε_s	Strain in longitudinal tension reinforcement
ε'_s	Strain in longitudinal compression reinforcement
ρ_{sv}	Ratio of volume of shear reinforcement to volume of concrete core measured to outside of Stirrups
ρ_w	Ratio of area of longitudinal reinforcement to beam effective sectional area

2. Proposed modified truss model approach

A graphical presentation of the overall configuration of the modified truss model is illustrated in Fig. 1. Compressive members are shown in dotted lines while tensile members are shown in solid lines. Particularly, the shear span of the RC beam is modeled by a statically indeterminate truss model with struts at various angles. In the middle portion of the truss where the moment is constant and the shear force is zero, two 2-dimensional elastic panels are thus used in the truss model without losing of any generality. Every element in the truss model will be illustrated in detail herein. The top chord members of the truss, which represent longitudinal top reinforcement and concrete, are modeled by idealized uniaxial fiber model according to To et al. [3] to simulate the axial force–displacement characteristics of a combined action of concrete and steel reinforcement. The longitudinal bottom chord members of the truss, which carry tensile force, are represented by longitudinal tension reinforcements only and concrete tensile contribution is ignored. The height of the modified truss model is standardized and defined to be the distance between the centroid of the top chord to the bottom tension reinforcement. The longitudinal top and bottom chord members of the truss are further connected by diagonal compression struts of the truss model that represent the cracked concrete in compression and transverse tension ties of the truss.

The compression struts and tension ties in the transverse direction are the primary mechanisms for shear transfer and resistance. The choice of the strut configurations needs reasonable justification. Considering equilibrium in the shear span of a beam, the moment resistance of the beam can be expressed by:

$$M = Tjd. \tag{1}$$

The contribution of the dowel force towards flexural resistance is neglected in Eq. (1). Combining Eq. (1) with the relation between the shear and rate of change of bending moment along a beam, the following modes of internal shear resistance result:

$$V = \frac{\mathrm{d}M}{\mathrm{d}x} = \frac{\mathrm{d}}{\mathrm{d}x}(Tjd) = jd\frac{\mathrm{d}T}{\mathrm{d}x} + T\frac{\mathrm{d}(jd)}{\mathrm{d}x}. \tag{2}$$

The first term of Eq. (2) expresses the behavior of a true flexural member in which the internal tensile force *T* acting on a constant lever arm *jd* changes from point to point along the beam. It is the equation for perfect "beam action". The second term of Eq. (2) is the extreme case that the bond between steel and concrete is destroyed over the entire length of the shear span. Under such circumstances the external shear can be resisted only by the inclined internal compression. This extreme case may be termed "arch action". In a normal RC beams, where the full bond force required for beam action cannot be developed, these two mechanisms offer a combined resistance against shear forces.

It is known that the arch action could also be an important mode of shear resistance. Hence, both the beam action and the arch action should be considered when modeling RC beam. The proposed modified truss model in this paper caters for the arch mechanism by introducing compression struts which directly connects the loading points with the supports. Meanwhile, the beam action is represented by diagonal compression struts with variable angles of inclination. This variable angle of inclination is achieved by dividing the shear span into four equal portions. Each portion of compression strut is then connected to the loading point in the lower portion or to the support in the upper portion as shown in Fig. 1. This simple y direct method to construct the truss with struts at various angles is found to be sufficient as the results will later show. Concrete contribution in the beam action is also included in these struts at various angles.

3. Properties of the modified truss model

Elements in truss model must have their material properties before the truss model can be further analyzed. In the proposed truss model, the stress–strain relationship for concrete follows the constitutive curve proposed by Kent and Park [5] as shown in Fig. 2. The equations governing the behavior are given below:

For region *AC*

$$f_c = f_c' \left[\frac{2\varepsilon_c}{0.002} - \left(\frac{\varepsilon_c}{0.002} \right)^2 \right]. \tag{3}$$

For region CD

$$f_c = f_c' \left[1 - Z\left(\varepsilon_c - 0.002\right)\right] \tag{4}$$

$$Z = \frac{0.5}{\varepsilon_{50u} + \varepsilon_{50h} - 0.002} \tag{5}$$

$$\varepsilon_{50u} = \frac{3 + 0.002 f_c'}{f_c' - 1000} \tag{6}$$

$$\varepsilon_{50h} = \frac{3}{4}\rho_{sv}\sqrt{\frac{b''}{s}}. \tag{7}$$

Here, the ascending parabola is simplified by bilinear sections *ABC* while the descending branch remains the same. The stress–strain relationship for reinforcing steel in Fig. 3 is bilinear and has a general strength-hardening ratio of 0.005. The yielding stress and strain of the reinforcement are specified from the experimental works accordingly.

Over the past 20 years, many researchers have concluded that the truss model analogy tends to overestimate the shear capacity and stiffness of RC beams when the failure stress of the concrete struts is assumed to be the uniaxial concrete compressive strength. Thus the stress that each type of concrete member can achieve should be carefully considered. In conventional flexural design theory, the uniaxial compression of concrete is assumed to prevail. The design concrete strength is taken to be $0.85f_c'$. The factor 0.85 considers the difference between the concrete cylinder strength and the strength of actual structures. Moreover, the compressive strength of concrete is affected by the presence of transverse stresses. In reality, a RC beam under flexure and shear is subjected to biaxial stress with tensile stresses with tensile stresses in the direction perpendicular to the principle compressive stresses. Therefore, the strength in the principal compressive direction is reduced by the principal tension perpendicular to it. This softened compressive stress is referred to as the “effective compressive stress of concrete” and is a function of certain factors. Considerable research has been conducted in an effort to determine the limiting concrete compressive stress. This paper adopted the suggestion from Schlaich et al. [6,7] for the effective stress of concrete. Therefore, $0.8f_c'$ is taken for the longitudinal chord concrete

element as parallel cracking with normal crack width. A compressive strength of $0.4f_c'$ is chosen for the diagonal compression struts to cater for skew cracks with extraordinary crack width. These reductions together with 0.85 make up the stress levels and then used to regulate the concrete member in the modified truss model.

Top chord members of the truss, consisting of top compression reinforcement and concrete stress block, are modeled by the uniaxial fiber element. The concrete area is defined as the compression zone. However, the center of the concrete stress block does not coincide with the center of top compression reinforcement. The concrete stress block will be transformed into an equivalent area centered at the center of top compression reinforcement by maintaining internal moment equilibrium as shown in Fig. 4. To accomplish this transformation computationally, it is assumed that the extreme fiber in the compressive concrete passes the strain at the maximum stress when the ultimate strength is reached and that the concrete stress block can be simplified as an equivalent rectangular stress distribution. This assumption is quite true as the concrete compressive strain at the maximum stress is quite small and can be achieved shortly after loading. Fig. 2 illustrates this transformation and the equivalent concrete area in the uniaxial fiber element. The sectional area of compression chord can then be derived as:

$$A_{cm} = \frac{\frac{A_s f_s}{0.85 f_c'}\left(d - \frac{A_s f_s}{1.7 f_c' b}\right)}{h} \times b. \tag{8}$$

Ideally, Eq. (8) gives the concrete area of each top chord member as long as f_s of the corresponding longitudinal bottom reinforcement is known. However, this is not very much operational as f_s, which is only obtainable from experimental strain gauge readings may not be available at every desired section. To overcome this disadvantage in the transformation, another equation is proposed from the view of flexure capacity that a top chord member can sustain. The top chord member of the truss must be able to sustain the ultimate moment demand at a reasonable stress state. From this consideration, the area of concrete in the top chord can be written as:

$$A_{cm} = \frac{M_u}{f_c' h}. \tag{9}$$

It should be noted that Eq. (9) does not consider any reduction in strength as the reduction factor will further increase the concrete area which makes the reduction in strength meaningless. In deriving Eqs. (8) and (9), the influence of top compression reinforcement is not included in the transformation as the area of top compression reinforcement is relatively small and is only subjected low strain in most beams. Furthermore, under the simplifications made in this paper, both Eqs. (8) and (9) give the maximum available concrete area for top chord members. For the longitudinal bottom chord elements, the properties are readily defined as the longitudinal bottom reinforcement in the position.

Next, the diagonal compression struts are discrete representation of the stress field inside the beams. One strut covers the stress flow in its nearby region. As the stress flow is continuous in a beam, the areas of the compression struts are determined from its geometrical consideration. An effective section l_b is defined on this basis for each strut; the sketch in Fig. 5 illustrates this concept. It can be seen that the area defined is actually the maximum allowable for each strut and this area is given as:

$$A_{sm} = l_b \times b. \tag{10}$$

The geometrical property of the arch member is calculated in the same way as described above together with the struts for beam action. The analytical results confirm that the arch action contribution for shear is highly related to this area determined herein. It should be also noted that maximum area is adopted for both concrete in top chord members and struts. Therefore, the behavior of these concrete members is reflected through the stress variations in them. It should be noted that these stresses are the average stresses within the members.

4. Concrete shear contribution

In a standard truss model illustrated in Fig. 6, one typical tension tie member *ij* in the transverse direction is formed by lumping all the stirrups cut across by section *A*–*A*. The compression strut that runs parallel to section *A*–*A* and connected to member *ij* transfers the force to the tension tie. If all stirrups reach yield when failure load is applied with all struts inclined at a same angle, the

distribution of stirrups would be considered ideal. Therefore, it is appropriate to assume that all the stirrups have yielded and each develops a force of $A_v f_y$. Based on these assumptions, the truss shown becomes statically determinate. From the equilibrium condition, the truss model capacity in shear V_s is obtained:

$$V_s = A_v f_y \frac{h}{s} \cot \alpha. \tag{11}$$

From this point of view, it can be seen that the shear resistance mechanism in the standard truss model mainly comes from the transverse ties or the stirrups. Hence, the truss model ignores the shear resistance components from the concrete contribution such as shear in the compression zone, aggregate interlock across crack, and the dowel action [8]. The modified truss model proposed herein works the same way as the standard truss model in principle when concrete shear contribution is null. This is again verified from an analysis of the proposed modified truss model for Beam S2-3 and S2-4 tested by Kong and Rangan [9] with no concrete contribution to shear resistance. Results shown in Fig. 7 clearly indicate that at the point of tension tie yielding, the shear capacity developed is significantly lower than the experimental ultimate strength (only 58% of the ultimate shear capacity). Also, the overall shear stiffness of the model is smaller than the test beam. A larger deflection is obtained for the modified truss model at the same level of shear force as compared with the experiment. Furthermore, due to the lower shear capacity, the ultimate deflection in the experiment cannot be achieved satisfactorily for the model without concrete shear contribution.

Thus, we conclude that a truss model without considering the concrete contribution in shear results in excessive conservation in both shear capacity and stiffness, and hence the deformation. The additional strength and stiffness required to capture the realistic behavior of the RC beams utilizing the truss model could only come from the shear resistance mechanism of the concrete contribution correctly incorporated. The importance of the inclusion of some of the components of the concrete shear failure mechanism to shear design has already been noted in the current ACI 318 design philosophy. ACI 318-02 [4] specifies this contribution as:

$$V_c = \left(0.16\sqrt{f_c'} + 17.2\rho_w \frac{V_u d}{M_u}\right) bd \leqslant 0.3\sqrt{f_c'} bd. \tag{12}$$

This additional term is a supplementary to the truss model that the ACI 318-02 code adopts.

A conceptual distribution between concrete shear contribution V_c and stirrup contribution V_s can be visualized in Fig. 8 [10]. The concrete contribution here remains constant throughout the monotonic loading process. This is justified for high strength concrete as the crack surface for high strength concrete is distinctly smoother [10,11], indicating that the subsequent effect of wearing off of the aggregate interlocking mechanism due to future loading is minimized. The dowel action is always present, unless the longitudinal reinforcement is broken apart. Therefore, the concrete contribution in shear can be reasonably recognized as a non-diminishing term in this analysis as Kong and Rangan [9] used high strength concrete in their experiment.

A truss model that works as a shear analytical tool relies on compression struts to transfer the shear force to the tension ties and the tension ties actually act against this force. So it has inherent difficulty in incorporating the concrete shear mechanism such as aggregate interlocking which is a shear resistance between struts and dowel action along the longitudinal reinforcement. Any other additional created member for concrete contribution into the truss model is not feasible. In this paper, an equivalent stirrup reinforcement ratio concept is proposed to deal with this problem in the modified truss model. Concrete contribution term V_c can be converted to the equivalent stirrup reinforcement with known yielding strength f_y.

$$A_{sc} = \frac{V_c}{f_y}. \tag{13}$$

The concrete contribution V_c in this paper follows the existing one in ACI 318-02 [4] (Eq. (12)). The yielding strength should be corresponding to that of the stirrups in the experiment. This equivalent steel area (Eq. (13)) is then uniformly distributed among the three ties that have been crossed by the struts for beam action. Finally, a tension tie should take into account both the distributed equivalent steel area and lump summed area from the shear reinforcement.

5. Experimental verification and discussion experimental and analytical validation

To validate the proposed truss models, a comparison with published experimental results with respect to the shear strength and load–deflection response obtained from test results is demonstrated. Using the complete methodology as introduced previously, a proposed truss model was set up for each beam according to its dimensions and detailing. Table 1 shows the details of the reinforced concrete beams. These beams encompass a wide range of cross sectional sizes, material properties, shear reinforcement ratios, longitudinal reinforcement ratios and shear span to effective depth ratios.

The modified truss models with established member properties are analyzed with the DRAIN-2DX code [12,13]. It was found that the average ratio of the predicted to experimental shear strength by the proposed model is 0.870 as shown in Table 2, showing a good correlation between the proposed model and experimental data. The shear strengths of beams in the database calculated based on ACI 318-02 [4] are also showed in Table 2. The mean ratio of the predicted to experimental strength and its coefficient of variation are 0.783 and 0.165, 0.870 and 0.158 for ACI 318-02 [4] and proposed model, respectively. Comparison of available models with experimental data indicates that proposed model produces better statistical correlation than the ACI 318-02 [4] model. The proposed model may be suitable as an assessment tool to calculate the shear strength of reinforced concrete beams which have similar detailing in the database.

The proposed truss models are also validated by plotting the analytical results in terms of shear force versus mid-span deflection response for a series of beams tested by Kong and Rangan [9] and comparing them with experimental data. The results are illustrated through Figs. 9–11. The proposed truss models demonstrate good reliability in these analyses. Reasonable matching of test and analysis curves is observed. One deficiency of the proposed truss model is that the predicted shear force versus mid-span deflection response curve is nearly linear. The stiffness in the initial loading stage is also small, compared to the experiment. This deficiency could be attributed to two reasons. Firstly, the concrete contribution is assumed to be constant throughout the loading and this would produce the

linear shear force versus mid-span deflection response. Secondly, the truss model analogy is strictly not applicable to the uncracked RC beams. If the truss model analogy is used for that range of loading, a smaller predicted stiffness is foreseeable.

The shear capacity of a RC beam is the key issue that is examined in the proposed truss model for each beam. Traditionally, the shear capacity of the truss model is attained when any one of the tension ties in the model yields. In the proposed truss model, yielding of the tension ties indicates that both concrete and stirrup in that position have fully participated in the shear resistance. Therefore, the shear capacity is reached too. The analytical results show that yielding is first observed at the second tension tie at the middle of each beam model under the current configuration of the modified truss model. This result corresponds well with Paulay's assumption for the variation of stirrup force intensity along the span of the coupling beam [2].

Further investigations were carried out to examine the internal stress distribution of the truss models for a series of beams tested by Kong and Rangan [9]. The stresses in each member of the proposed truss models are shown through Figs. 12–14. For concrete members, the stresses are expressed in term of f_c' , while the stresses for steel members are expressed in term of f_y. Crack patterns are shown in dotted line for easy comparison.

All tested beams failed in shear. As such, the proposed truss models for the tested beams also demonstrated distinct shear governing behavior with the stirrups reaching yield first. Flexural longitudinal reinforcement for all truss models is well below yielding point at every position along the shear span of the tested beams. Stress for the top chord concrete member, however, varied in a fluctuating manner. This is due to the member area, which depends on the ultimate moment capacity from the experiment as determined from Eq. (9). However, the available experimental data were not consistent in some cases. For tension ties, as discussed above, the yielding starts at the second tie from the center. The other two ties are of moderate stress level ranging from 60% to 70% of f_y, respectively. Reduction factors work well for concrete members as the stresses in these members did not exceed the limited values. For the concrete in the top chord members, the reduction is approximately $0.72f_c'$ and the maximum average stress reached by all modified truss models is around $0.40f_c'$. For struts, the reduction

is approximately $0.34f_c'$ and the maximum average stress for these members is around $0.25f_c'$. This value is lower than that specified and thus the web crushing failure is prevented. This correlates well with the current design practice which requires that failure due to concrete crushing prior to yielding of the reinforcement is avoided with the use of the truss model approach within the general ductile framework.

6. Parametric analyses

The test parameters are the shear reinforcement ratio, longitudinal reinforcement ratio, and shear span to effective depth ratio can be reflected from the internal stress analysis of the proposed truss models. For tested beams S2-1, S2-2, S2-3, S2-4, and S2-5, (see Fig. 9) the shear reinforcement ratio varied decreasingly with the spacing of the stirrups. With the increase in shear reinforcement ratio, the shear capacity of the beams increased as expected in the modified truss models. Fig. 15 clearly shows this trend when compared with experimental data. Stress of the longitudinal reinforcement also increases as more stirrup content enhances shear capacity and shifts the behavior of the beams towards a flexural domain. More stirrup content does provide a confinement effect on the concrete core, enhancing the performance of the compression struts. Thus, compression struts develop higher stresses with the increase of stirrup content. It is noteworthy that the shear force carried by the arch action remains relatively constant with the increase of the shear reinforcement ratio.

For the tested beams S3-1, S3-2, S3-3, S3-4, S3-5, and S3-6 (see Fig. 10), the proposed model underestimates the shear strength of reinforced concrete beams with high longitudinal reinforcement ratio (see Fig. 16). However, the stresses of the longitudinal bottom chord members demonstrate a decreasing trend as the ratio goes higher. On the other hand, stresses in the compression struts also build up. Especially for the arch members, the stresses go up at a faster rate and eventually become the critical element among all the compression struts.

Beams S5-1, S5-2, and S5-3 had a constant effective depth while their respective shear-span decreased which resulted in a decrease in the shear span to effective depth ratio *a/d*. The behavior of shear domain is more pronounced with the decrease of shear span to an effective

depth ratio. This is proven by the decreasing trend of the flexural longitudinal reinforcement stresses. Also, the shear capacity goes up for this series of beams, but the rate is rather gentle as shown in Fig. 17. It is also found that the stresses of the struts catering for the beam action reduce with a lower shear span to an effective depth ratio. However, stresses in the arch members build up significantly as the ratio decreases.

7. Limitations and recommendations

According to the findings of the present study, the usage of the proposed truss model in the prediction of the load–deflection response and shear strength of RC beams can be improved in four aspects. Firstly, the treatment of the concrete contribution as a non-diminishing term in the analysis is an insufficient simplification as this will lead to near linear behavior in terms of load–deflection response. In addition, the non-linear degrading branch of load–deflection response could not be modeled by assuming a non-diminishing concrete contribution. Concrete contribution can be possibly taken as a variable during the whole loading process. Secondly, the inclination of the diagonal struts is very much predefined when forming the modified truss model. A more rigorous procedure can be developed to overcome this limitation. Thirdly, the proposed truss model assumed the existence of both "beam action" and "arch action". Hence, the proposed truss model is only applicable for reinforced concrete beams with aspect ratio, a/d in range of 2–3 where both "beam action" and "arch action" prevail. Other models could be developed for reinforced concrete beams with high and low aspect ratios. Fourthly, the proposed truss model is an analytical tool to understanding the mechanisms of RC beams subjected to flexure and shear. Due to its indeterminate nature, it can only have limited usage in design. An approach with variable angle truss model enabling hand calculation for strength and stiffness is needed. It is concluded that further researches should focus on these aspects to further improve the proposed truss model.

8. Conclusions

The study presented in this paper provides a systematic development of a truss model that can be used to predict the load–deflection response of a cracked RC beam subjected to shear and

flexure. It was found from this study that even the truss model with struts at various angles which only utilizes stirrup as the shear resistance mechanism, is not sufficient to model the primary mechanism of shear resistance. On this basis, the proposed truss model did provide a concept of equivalent stirrup reinforcement to deal with the concrete shear contribution. With these considerations, the modified truss model enables researchers to predict the load–deflection response of RC beams subjected to shear and flexure without excessive conservation. The predicted shear strengths and load–deflection responses correlated fairly well with the available experimental data, with the exception of a few specimens. Furthermore, the truss model analogy, or particularly the modified truss model proposed herein, can demonstrate clearly the stress distributions in various members within the truss. This results in a better understanding of the resistance and failure mechanisms in RC beams subjected to shear and flexure.

References

[1] Bresler B, MacGregor JG. Review of concrete beams failing in shear. ACI J Proc 1967;93(1):343–72.

[2] Paulay T. Coupling beams of RC shear walls. J Struct Div, ASCE 1971; 97ST3(March):843–62.

[3] To NHT, Ingham JM, Sritharan S. Cyclic strut-and-tie modeling of simple RC structures. In: Proceedings of 12 WCEE, 2000, p. 1249.

[4] ACI Committee 318, Building code requirements for structural concrete (ACI 318-02) and commentary (ACI 318R-02), American Concrete Institute, Farming Hills, MI, 2002.

[5] Park R, Paulay T. RC structures, New York: John Wiley and Sons.

[6] Schlaich J, Schafer K. Designs and detailing of structural concrete using strut-and-tie models. The Struct Eng 1991;69(6):113–25.

[7] Schlaich J, Schäfer K, Jennewein M. Toward a consistent design of structural concrete. PCI J 1987;32(3):74–150.

[8] MacGregor JG, Bartlett FM. RC : Mechanics and design. first Canadian edition. Scarborough (Ontario): Prentice-Hall Canada Inc; 2000. p. 173–300.

[9] Kong PYL, Rangan BV. Shear strength of high-performance concrete beams. ACI Struct J 1998;95(6):677–87.

[10] Pendyala RS, Mendis P. Experimental study on shear strength of high-strength concrete beams. ACI Struct J 2000;97(4):564–71.

[11] Elzanaty AH, Nilson AH, Slate FO. Shear shear of RC beams using high-strength concrete. ACI J Proc 1986;81(2):290–6.

[12] Powell GH. DRAIN-2DX element description and user guide for element Type 01, Type 02, Type 04, Type 06, Type 09 and Type 15 Version1.10. Report No. UCB/SEMM-93/18. Berkeley (CA): Department of Civil Engineering, University of California.

[13] Prakash V, Powell GH, Campbell S. DRAIN-2DX base program description and user guide version 1.01. Report No. UCB/SEMM-93/17. Berkeley (CA): Department of Civil Engineering, University of California.

[14] Tompos EJ, Frosch RJ. Influence of beam size, longitudinal reinforcement, and stirrup effectiveness on concrete shear strength. ACI Struct J 2002;99(5): 559–67.

[15] Rahal KN, Al-Shaleh KS. Minimum transverse reinforcement in 65Mpa concrete beams.

ACI Struct J 2004;101(6):872–8.

[16] Rahal KN. Shear behavior of reinforced concrete beams with variable thickness of concrete side cover. ACI Struct J 2006;103(2):171–7.

[17] Ozcebe G, Ersoy U, Tankut T. Evaluation of minimum shear reinforcement requirements for higher strength concrete. ACI Struct J 1999;96(3):361–9.

[18] Johnson MK, Ramirez JA. Minimum shear reinforcement in beams with high strength concrete. ACI Struct J 1989;86(4):376–82.

[19] Naravanan R, Darwish IYS. Use of steel fibers as shear reinforcement. ACI Struct J 1988;84(3):216–27.

List of Tables

List of Figures

	Beam mark	Beam						Shear reinforcement			Longitudinal reinforcement		
		f'_c (MPa)	h (mm)	b (mm)	d (mm)	a (mm)		Diameter (mm)	Spacing (mm)	f_y (MPa)	Top (mm^2)	Bottom (mm^2)	f_y (MPa)
Kong [9]	S2-1	72.5	350	250	292	730	2.50	5.0 (2)	150	569	224	2046	452
	S2-2	72.5	350	250	292	730	2.50	5.0 (2)	125	569	224	2046	452
	S2-3	72.5	350	250	292	730	2.50	5.0 (2)	100	569	224	2046	452
	S2-4	72.5	350	250	292	730	2.50	5.0 (2)	100	569	224	2046	452
	S2-5	72.5	350	250	292	730	2.50	5.0 (2)	75	569	224	2046	452
	S3-1	67.4	350	250	297	740	2.49	4.0 (2)	100	632	224	1232	450
	S3-2	67.4	350	250	297	740	2.49	4.0 (2)	100	632	224	1232	450
	S3-3	67.4	350	250	293	730	2.49	4.0 (2)	100	632	224	2046	452
	S3-4	67.4	350	250	293	730	2.49	4.0 (2)	100	632	224	2046	452
	S3-5	67.4	350	250	299	720	2.41	4.0 (2)	100	632	224	2760	442
	S3-6	67.4	350	250	299	720	2.41	4.0 (2)	100	632	224	2760	442
	S5-1	89.4	350	250	292	880	3.01	5.0 (2)	100	569	224	2046	452
	S5-2	89.4	350	250	292	800	2.74	5.0 (2)	100	569	224	2046	452
	S5-3	89.4	350	250	292	730	2.50	5.0 (2)	100	569	224	2046	452
Tompos [14]	V36-2	27.5	915	457	852	2553	3.0	6.4 (2)	165	483	125	3847	482
	V36-3	27.5	915	457	852	2553	3.0	9.4 (2)	371	483	125	3847	482
	V18-2	27.5	486	229	425	1276	3.0	6.4 (2)	186	538	145	1013	552
	V18-2c	27.5	486	229	425	1276	3.0	6.4 (2)	186	538	145	1013	552
Rahal [15]	A65-140	62.1	370	200	320	900	2.8	6.0 (2)	140	240	229	1473	440
	A65-110	60.9	370	200	320	900	2.8	6.0 (2)	110	240	229	1473	440
	A65-95	62.1	370	200	320	900	2.8	6.0 (2)	95	240	229	1473	440
	B65-140	65.1	370	200	320	900	2.8	6.0 (2)	140	305	229	2457	440
	B65-125	66.4	370	200	320	900	2.8	6.0 (2)	125	305	229	2457	440
	B65-110	66.4	370	200	320	900	2.8	6.0 (2)	110	305	229	2457	440
Rahal [16]	S3-25-50	27.3	400	300	340	1020	3.0	8.0 (2)	170	445	312	1968	440
	S3-25-75	25.3	400	350	340	1020	3.0	8.0 (2)	170	445	312	1968	440
	S3-40-50	41.6	400	300	340	1020	3.0	8.0 (2)	170	445	312	1968	440
	S3-40-75	42.2	400	350	340	1020	3.0	8.0 (2)	170	445	312	1968	440
Ozcebe [17]	S-59-ACI	73.0	360	150	325	975	3.0	4.0 (2)	120	255	157	2057	410
	S-59-TH	73.0	360	150	325	975	3.0	4.0 (2)	80	255	157	2057	410
	S-59-TS	73.0	360	150	325	975	3.0	4.0 (2)	60	255	157	2057	410
Johnson [18]	Beam 7	51.3	610	305	550	1670	3.0	6.0 (2)	267	479.2	1284	4093	524.7
	Beam 5	55.8	610	305	550	1670	3.0	6.0 (2)	133	479.2	1284	4093	524.7
Naravanan [19]	SS4	43.3	150	85	131	262	2.0	3.0 (2)	80	320	116	254	530

Table 1

	Beam Mark	V_u (kN)	V (kN)	V_p (ACI) (kN)	$\frac{V}{V_u}$	$\frac{V_p}{V_u}$
Kong [9]	S2-1	260.3	199.4	166.4	0.766	0.639
	S2-2	232.5	212.9	175.1	0.916	0.753
	S2-3	253.3	231.0	188.2	0.911	0.743
	S2-4	219.4	231.0	188.2	1.053	0.858
	S2-5	282.1	257.6	209.9	0.913	0.744
	S3-1	209.2	170.1	158.9	0.813	0.760
	S3-2	178.0	170.1	158.9	0.956	0.893
	S3-3	228.6	210.0	166.4	0.917	0.728
	S3-4	174.9	210.0	166.4	1.201	0.951
	S3-5	296.6	225.6	179.3	0.761	0.606
	S3-6	282.9	225.6	179.3	0.797	0.634
	S5-1	241.7	221.8	193.2	0.918	0.799
	S5-2	259.9	230.0	195.7	0.885	0.753
	S5-3	243.8	242.4	199.1	0.994	0.817
Tompos [14]	V36-2	487.5	512.5	514.4	1.051	1.055
	V36-3	511.5	512.5	514.4	1.002	1.006
	V18-2	172.1	186.2	175.1	1.082	1.017
	V18-2c	153.0	186.2	175.1	1.217	1.144
Rahal [15]	A65-140	150.0	120.0	117.1	0.800	0.780
	A65-110	188.0	134.2	124.8	0.714	0.663
	A65-95	220.0	141.8	132.0	0.645	0.600
	B65-140	235.0	145.3	112.2	0.618	0.477
	B65-125	242.0	148.4	116.8	0.613	0.483
	B65-110	270.0	157.3	121.5	0.583	0.450
Rahal [16]	S3-25-50	199.0	192.1	200.2	0.965	1.006
	S3-25-75	244.0	227.0	210.8	0.930	0.864
	S3-40-50	262.0	237.8	220.3	0.908	0.841
	S3-40-75	264.0	255.0	238.6	0.966	0.904
Ozcebe [17]	S-59-ACI	111.8	92.9	97.4	0.831	0.872
	S-59-TH	142.9	105.6	107.0	0.749	0.749
	S-59-TS	179.2	119.4	116.7	0.666	0.651
Johnson [18]	Beam 7	317.0	276.2	279.1	0.871	0.880
	Beam 5	433.0	370.8	338.5	0.856	0.782
Naravanan [19]	SS4	32.0	22.3	23.0	0.696	0.719
				Average	0.870	0.783
				COV	0.158	0.165

Table 2

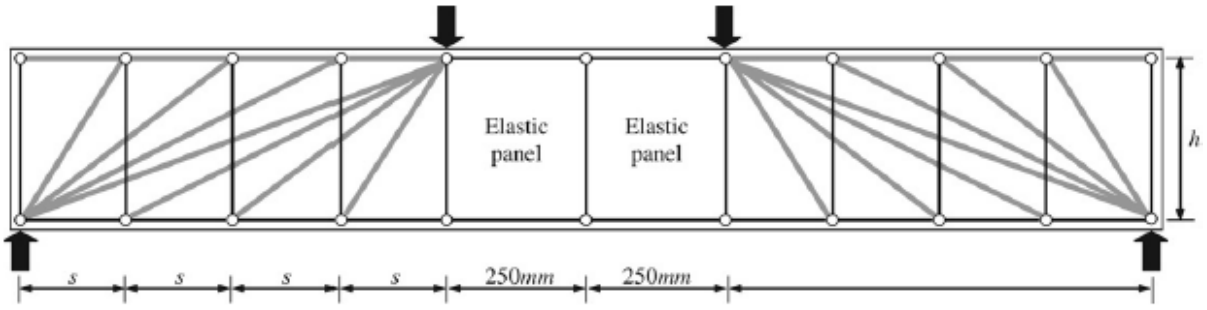

Fig. 1

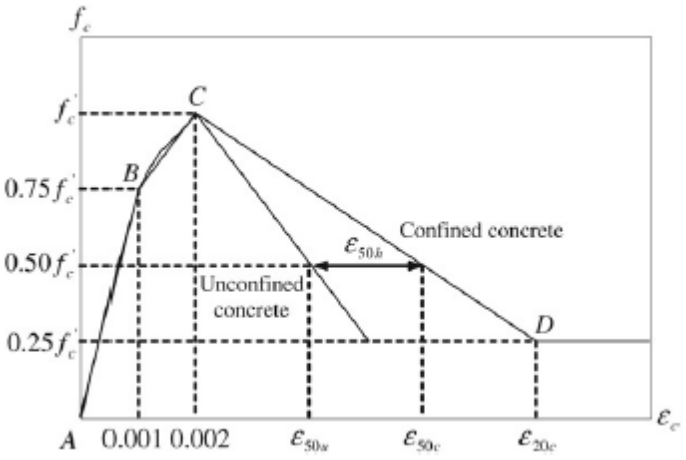
f_c
f_c'
$0.75f_c'$
$0.50f_c'$
$0.25f_c'$
C
B
D
A
Confined concrete
$\varepsilon_{50,h}$
Unconfined concrete
0.001 0.002
ε_{50u}
ε_{50c}
ε_{20c}
ε_c

Fig. 2

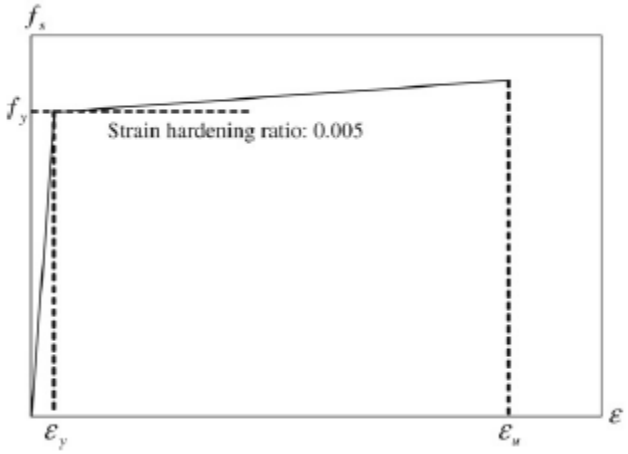
f_s
f_y
Strain hardening ratio: 0.005
ε_y
ε_u
ε

Fig. 3

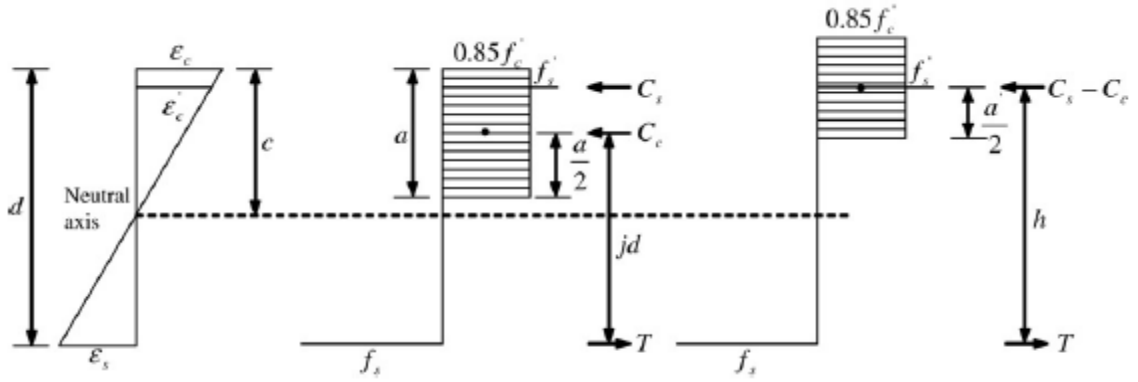
ε_c
ε_c'
d
Neutral axis
c
ε_s
$0.85f_c'$
f_s'
C_s
a
C_c
$\frac{a}{2}$
jd
T
f_s
$0.85f_c'$
f_s'
$\frac{a'}{2}$
$C_s - C_c$
h
T
f_s

Fig. 4

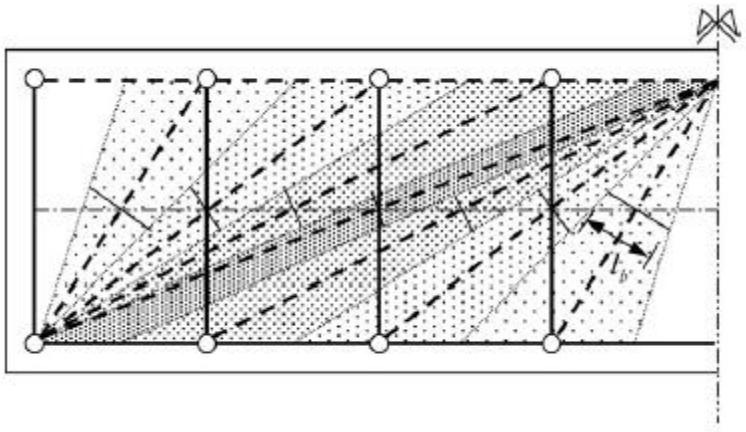

Fig. 5

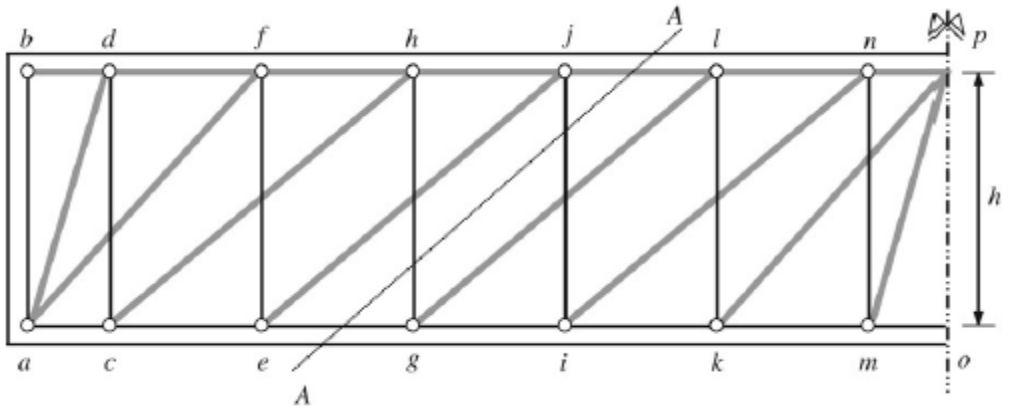

Fig. 6

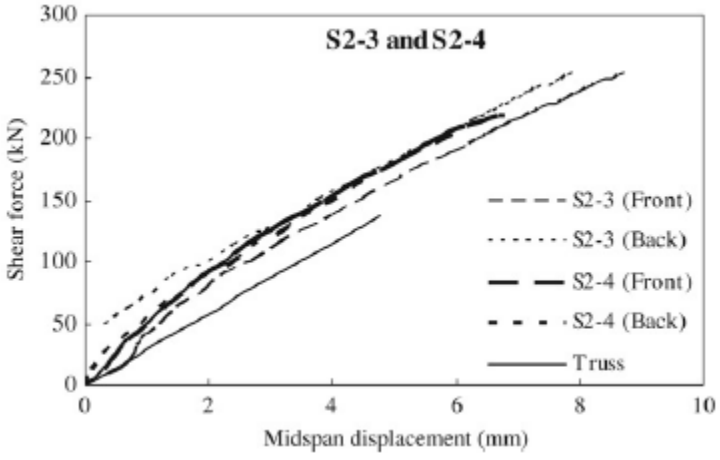
S2-3 and S2-4
Shear force (kN)
Midspan displacement (mm)
S2-3 (Front)
S2-3 (Back)
S2-4 (Front)
S2-4 (Back)
Truss
0
50
100
150
200
250
300
0
2
4
6
8
10

Fig. 7

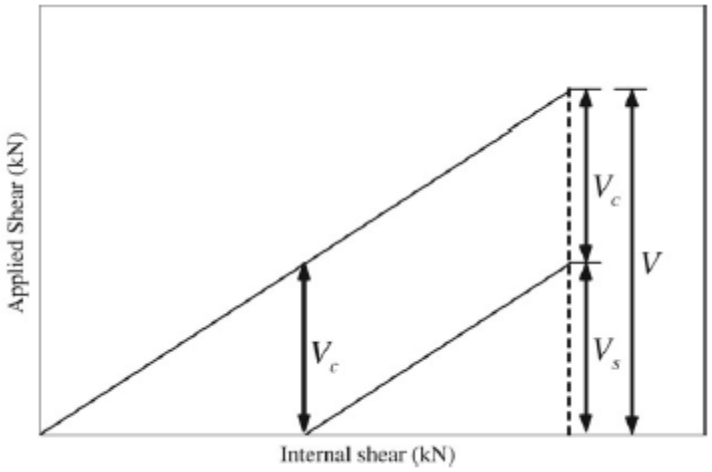

Fig. 8

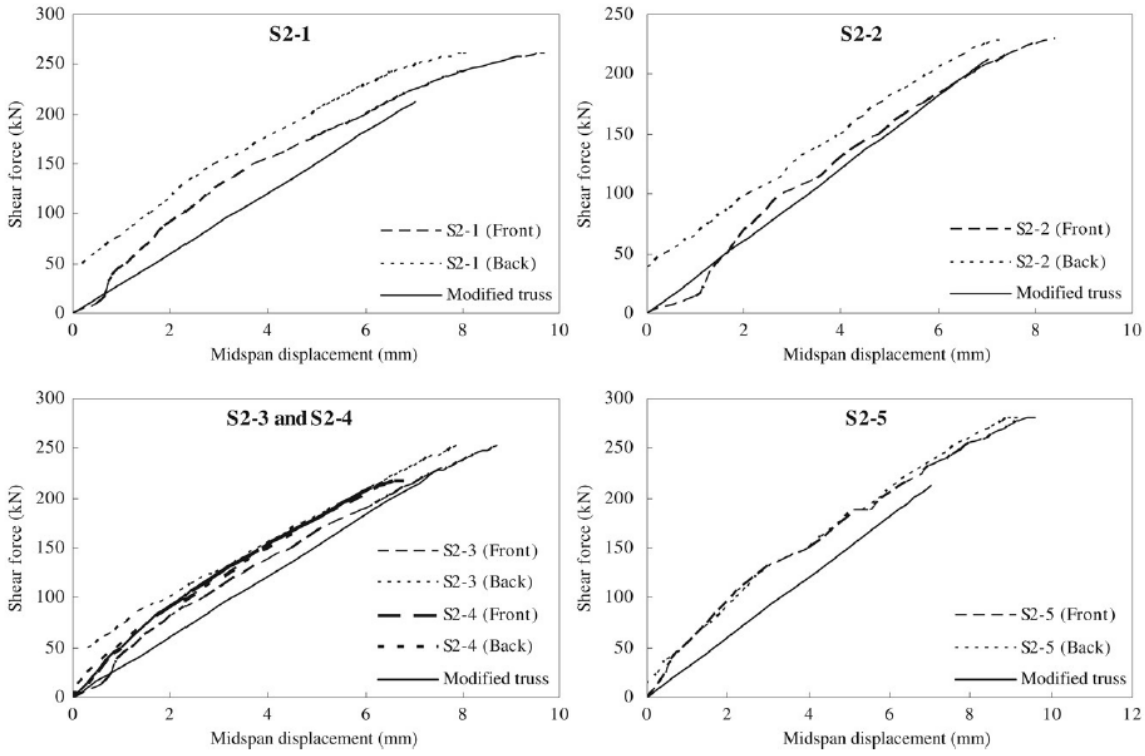
S2-1
Shear force (kN)
Midspan displacement (mm)
S2-1 (Front)
S2-1 (Back)
Modified truss
S2-2
Shear force (kN)
Midspan displacement (mm)
S2-2 (Front)
S2-2 (Back)
Modified truss
S2-3 and S2-4
Shear force (kN)
Midspan displacement (mm)
S2-3 (Front)
S2-3 (Back)
S2-4 (Front)
S2-4 (Back)
Modified truss
S2-5
Shear force (kN)
Midspan displacement (mm)
S2-5 (Front)
S2-5 (Back)
Modified truss

Fig. 9

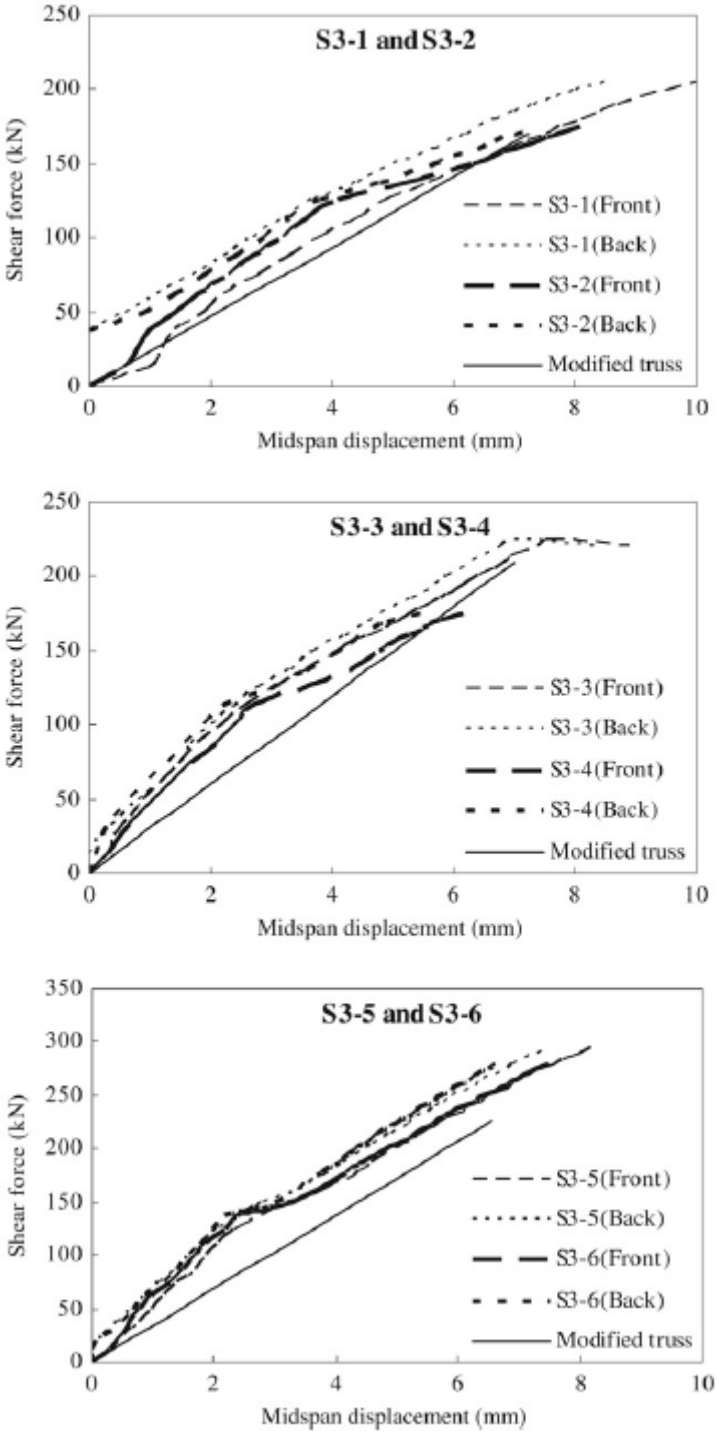
S3-1 and S3-2
Shear force (kN)
Midspan displacement (mm)
S3-1(Front)
S3-1(Back)
S3-2(Front)
S3-2(Back)
Modified truss
S3-3 and S3-4
Shear force (kN)
Midspan displacement (mm)
S3-3(Front)
S3-3(Back)
S3-4(Front)
S3-4(Back)
Modified truss
S3-5 and S3-6
Shear force (kN)
Midspan displacement (mm)
S3-5(Front)
S3-5(Back)
S3-6(Front)
S3-6(Back)
Modified truss

Fig. 10

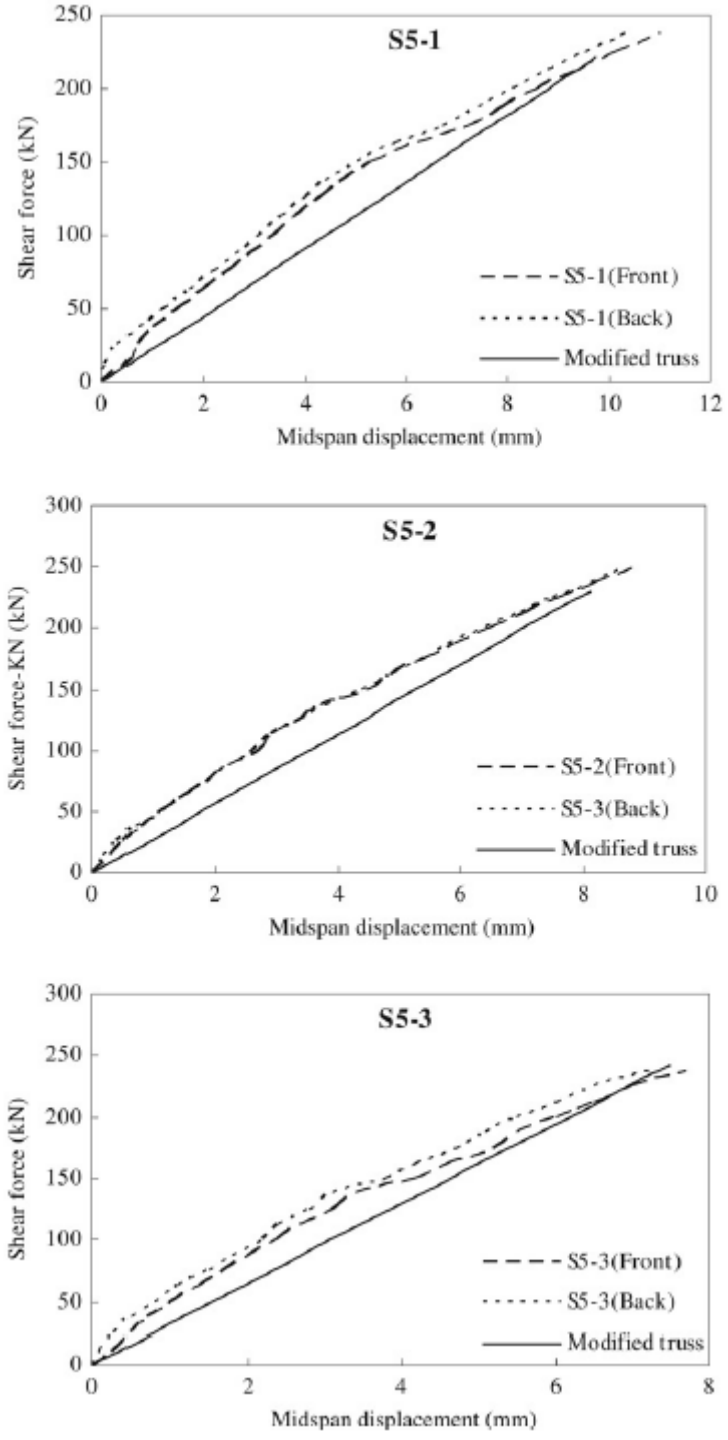
S5-1
Shear force (kN)
Midspan displacement (mm)
S5-1(Front)
S5-1(Back)
Modified truss
S5-2
Shear force-KN (kN)
Midspan displacement (mm)
S5-2(Front)
S5-3(Back)
Modified truss
S5-3
Shear force (kN)
Midspan displacement (mm)
S5-3(Front)
S5-3(Back)
Modified truss

Fig. 11

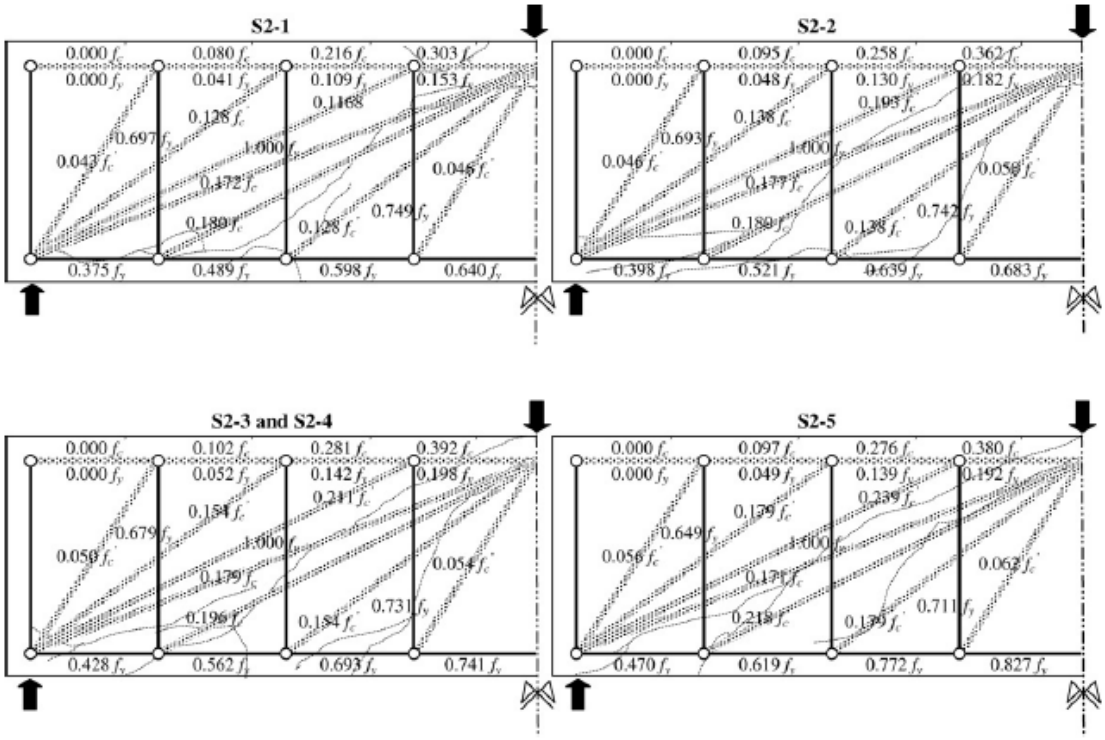
S2-1
0.000 f_c
0.080 f_c
0.216 f_c
0.303 f_c
0.000 f_y
0.041 f_y
0.109 f_y
0.153 f_y
0.128 f_c
0.1468
0.697 f_y
0.043 f_c
1.000 f_c
0.046 f_c
0.172 f_c
0.749 f_y
0.180 f_c
0.128 f_c
0.375 f_y
0.489 f_y
0.598 f_y
0.640 f_y
S2-2
0.000 f_c
0.095 f_c
0.258 f_c
0.362 f_c
0.000 f_y
0.048 f_y
0.130 f_y
0.182 f_y
0.138 f_c
0.193 f_c
0.693 f_y
0.046 f_c
1.000 f_c
0.059 f_c
0.177 f_c
0.742 f_y
0.189 f_c
0.138 f_c
0.398 f_y
0.521 f_y
0.639 f_y
0.683 f_y
S2-3 and S2-4
0.000 f_c
0.102 f_c
0.281 f_c
0.392 f_c
0.000 f_y
0.052 f_y
0.142 f_y
0.198 f_y
0.154 f_c
0.241 f_c
0.679 f_y
0.050 f_c
1.000 f_c
0.054 f_c
0.179 f_c
0.731 f_y
0.196 f_c
0.184 f_c
0.428 f_y
0.562 f_y
0.693 f_y
0.741 f_y
S2-5
0.000 f_c
0.097 f_c
0.276 f_c
0.380 f_c
0.000 f_y
0.049 f_y
0.139 f_y
0.192 f_y
0.139 f_c
0.239 f_c
0.649 f_y
0.056 f_c
1.000 f_c
0.062 f_c
0.171 f_c
0.711 f_y
0.218 f_c
0.136 f_c
0.470 f_y
0.619 f_y
0.772 f_y
0.827 f_y

Fig. 12

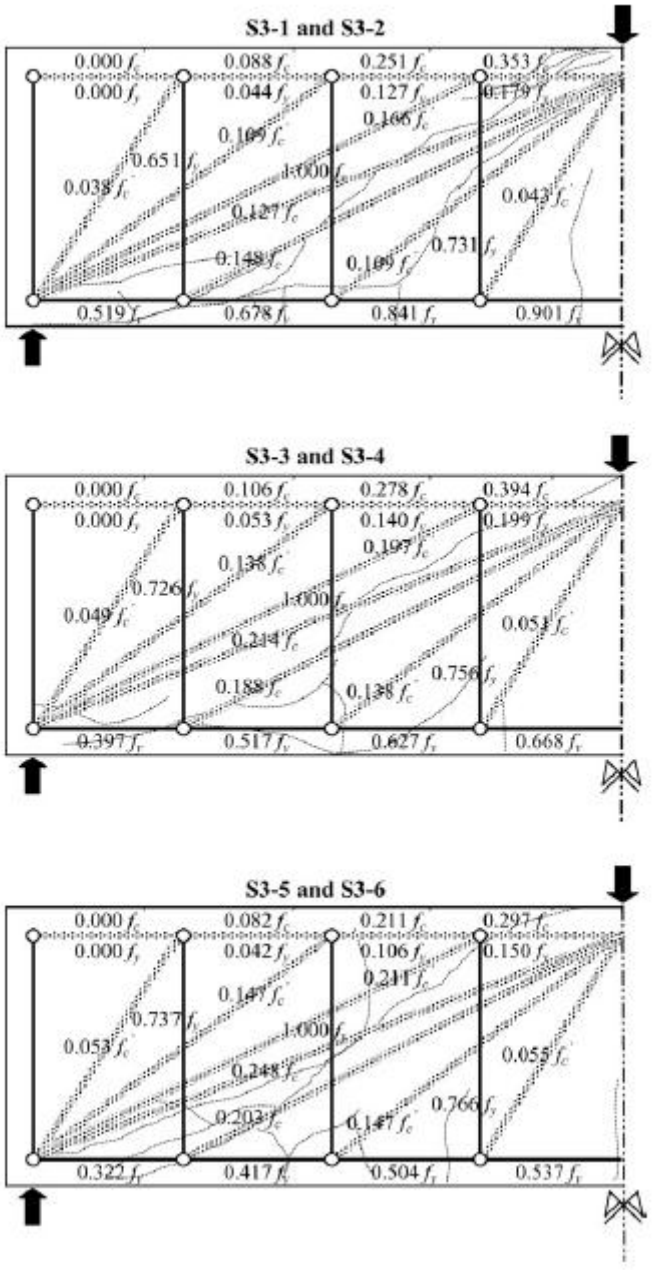
S3-1 and S3-2
0.000 f_c
0.088 f_c
0.251 f_c
0.353 f_c
0.000 f_y
0.044 f_y
0.127 f_y
0.179 f_y
0.166 f_c
0.109 f_c
0.651 f_y
1.000 f_y
0.038 f_c
0.043 f_c
0.127 f_c
0.731 f_y
0.148 f_c
0.109 f_c
0.519 f_y
0.678 f_y
0.841 f_y
0.901 f_y
S3-3 and S3-4
0.000 f_c
0.106 f_c
0.278 f_c
0.394 f_c
0.000 f_y
0.053 f_y
0.140 f_y
0.199 f_y
0.197 f_c
0.138 f_c
0.726 f_y
1.000 f_y
0.049 f_c
0.053 f_c
0.214 f_c
0.756 f_y
0.188 f_c
0.138 f_c
0.397 f_y
0.517 f_y
0.627 f_y
0.668 f_y
S3-5 and S3-6
0.000 f_c
0.082 f_c
0.211 f_c
0.297 f_c
0.000 f_y
0.042 f_y
0.106 f_y
0.150 f_y
0.211 f_c
0.147 f_c
0.737 f_y
1.000 f_y
0.053 f_c
0.055 f_c
0.248 f_c
0.766 f_y
0.203 f_c
0.147 f_c
0.322 f_y
0.417 f_y
0.504 f_y
0.537 f_y

Fig. 13

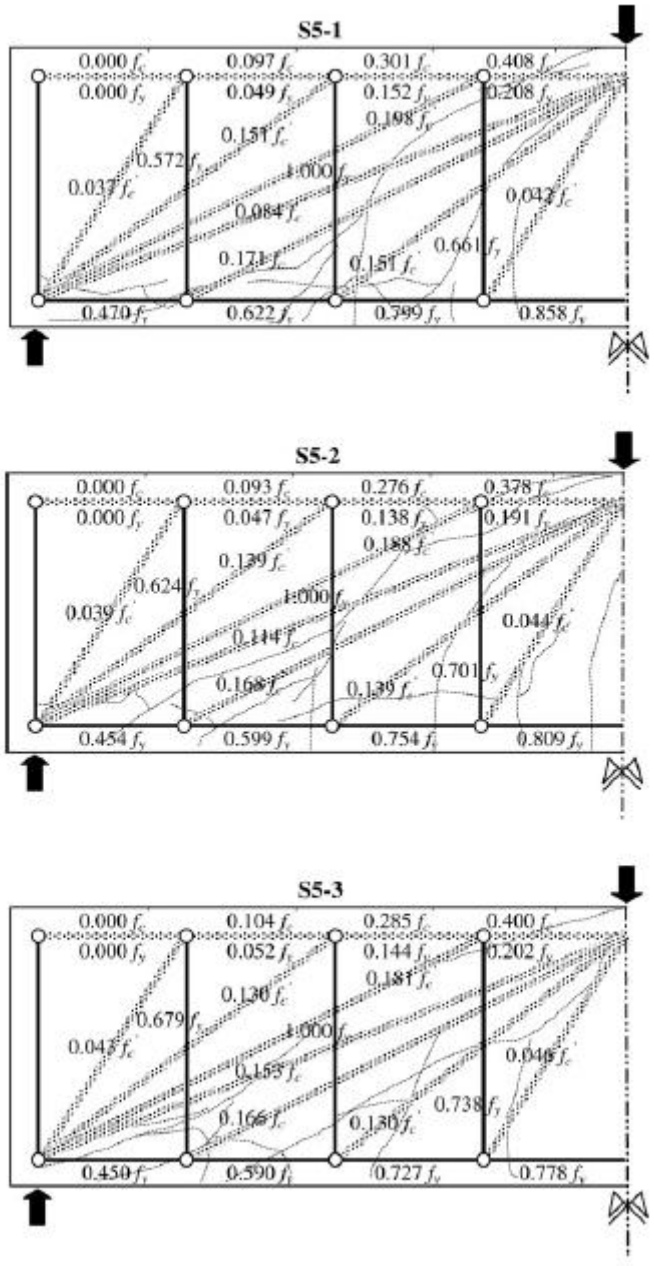
S5-1
0.000 f_c
0.097 f_c
0.301 f_c
0.408 f_c
0.000 f_y
0.049 f_y
0.152 f_y
0.208 f_y
0.198 f_y
0.151 f_c
0.572 f_y
1.000 f_y
0.037 f_c
0.084 f_c
0.042 f_c
0.661 f_y
0.171 f_c
0.151 f_c
0.470 f_y
0.622 f_y
0.789 f_y
0.858 f_y
S5-2
0.000 f_c
0.093 f_c
0.276 f_c
0.378 f_c
0.000 f_y
0.047 f_y
0.138 f_y
0.191 f_y
0.188 f_c
0.139 f_c
0.624 f_y
1.000 f_y
0.039 f_c
0.044 f_c
0.114 f_c
0.701 f_y
0.139 f_c
0.454 f_y
0.599 f_y
0.754 f_y
0.809 f_y
S5-3
0.000 f_c
0.104 f_c
0.285 f_c
0.400 f_c
0.000 f_y
0.052 f_y
0.144 f_y
0.202 f_y
0.181 f_c
0.130 f_c
0.679 f_y
1.000 f_y
0.043 f_c
0.046 f_c
0.155 f_c
0.738 f_y
0.166 f_c
0.130 f_c
0.450 f_y
0.590 f_y
0.727 f_y
0.778 f_y

Fig. 14

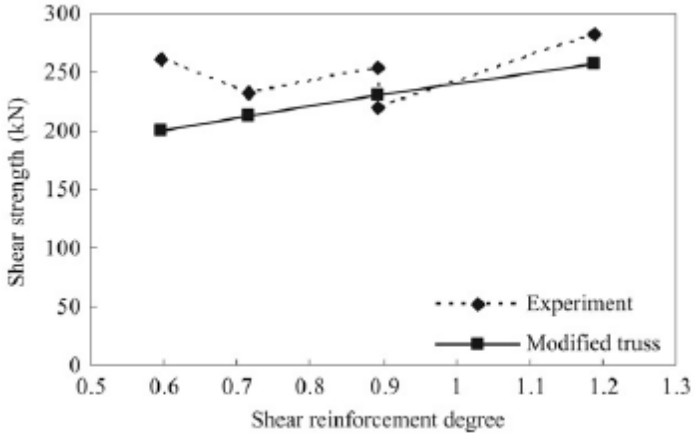
300
250
200
150
100
50
0
Shear strength (kN)
0.5
0.6
0.7
0.8
0.9
1
1.1
1.2
1.3
Shear reinforcement degree
Experiment
Modified truss

Fig. 15

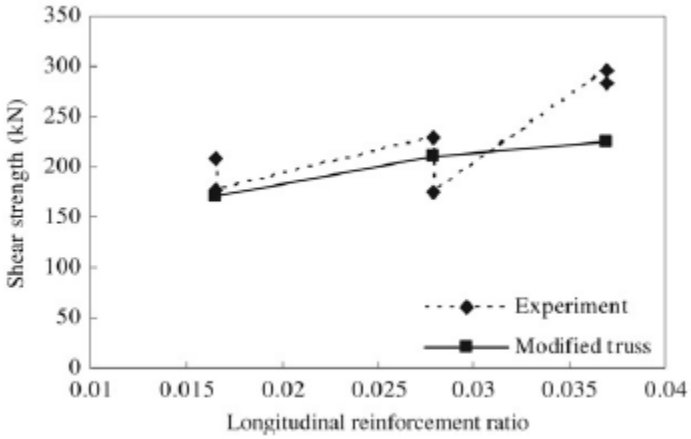
350
300
250
200
150
100
50
0
Shear strength (kN)
0.01
0.015
0.02
0.025
0.03
0.035
0.04
Longitudinal reinforcement ratio
Experiment
Modified truss

Fig. 16

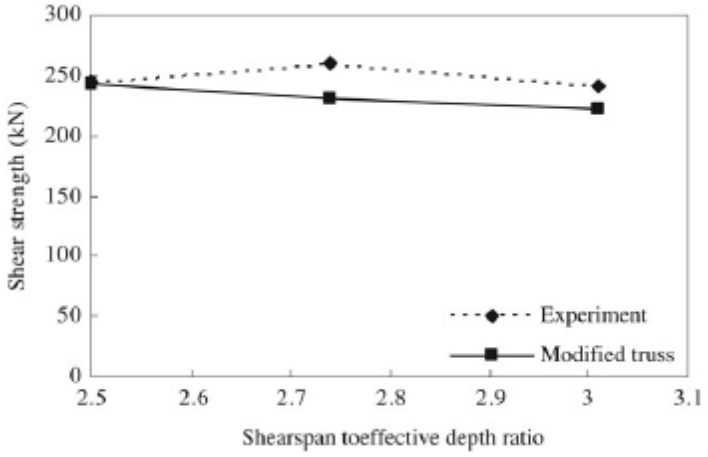
300
250
200
150
100
50
0
Shear strength (kN)
2.5
2.6
2.7
2.8
2.9
3
3.1
Shearspan toeffective depth ratio
Experiment
Modified truss

Fig. 17